

Isotopic lithium abundances in five metal-poor disk stars *

P.E. Nissen¹, D.L. Lambert², F. Primas³, and V.V. Smith⁴

¹ Institute of Physics and Astronomy, University of Aarhus, DK-8000 Aarhus C, Denmark

² Department of Astronomy, University of Texas, Austin, TX 78712-1083

³ European Southern Observatory, Karl-Schwarzschild Str. 2, D-85748 Garching b. München

⁴ Department of Physics, University of Texas at El Paso, El Paso, TX 79968-0515

Received 15 April 1999 / Accepted June 1 1999

Abstract. High resolution ($R \simeq 110\,000$), very high S/N spectra centered on the 6707.8 Å Li I line have been obtained with the ESO Coudé Echelle Spectrometer for five, metal-poor ($-0.8 < [\text{Fe}/\text{H}] < -0.6$) disk stars in the turnoff region of the HR-diagram. The instrumental and stellar atmospheric line broadening have been determined from two unblended iron lines and used in a model atmosphere synthesis of the profile of the Li I line as a function of the lithium isotope ratio. This has led to a detection of ${}^6\text{Li}$ in HD 68284 and HD 130551 with ${}^6\text{Li}/{}^7\text{Li} \simeq 0.05$, whereas the other stars, HR 2883, HR 3578 and HR 8181, have ${}^6\text{Li}/{}^7\text{Li}$ close to zero.

By comparing T_{eff} -values and absolute magnitudes based on Hipparcos parallaxes with recent stellar evolutionary tracks, the masses of the stars have been derived. It is shown that the two stars with ${}^6\text{Li}$ present have a significantly higher mass, $\mathcal{M}/\mathcal{M}_{\odot} \simeq 1.05$, than the other three stars for which values between 0.85 and 1.0 \mathcal{M}_{\odot} are obtained.

The results are discussed in terms of models for the galactic evolution of the light elements and depletion of the lithium isotopes in stellar envelopes. It is shown that the measured ${}^6\text{Li}$ abundances are in agreement with standard cosmic ray production of ${}^6\text{Li}$ in the galactic disk and a moderate depletion (0.5 dex) in the stars. Recent models for the evolution of ${}^6\text{Li}$ including $\alpha + \alpha$ fusion reactions and predicting a high lithium isotopic ratio, ${}^6\text{Li}/{}^7\text{Li} \simeq 0.3$ at $[\text{Fe}/\text{H}] = -0.6$, require a high degree of ${}^6\text{Li}$ depletion ($\simeq 1.0$ dex) to fit the observations. Furthermore, these models imply a ${}^7\text{Li}$ abundance about 0.2 dex higher than observed for metal-poor disk stars.

Key words: Stars: abundances – Stars: atmospheres – Stars: fundamental parameters – Stars: interiors – (ISM:) cosmic rays

1. Introduction

Measurements of the abundance of the ${}^6\text{Li}$ isotope in stellar atmospheres are of considerable interest and have attracted much attention since the first detection of ${}^6\text{Li}$ in the metal-poor turnoff star HD 84937 by Smith et al. (1993). The reason for this interest is threefold:

i) Detection of ${}^6\text{Li}$ in halo turnoff stars puts strong limits on the possible depletion of ${}^7\text{Li}$, and thus allows better determination of the primordial ${}^7\text{Li}$ abundance from the observed Li abundance of stars on the ‘Spite plateau’ (Copi et al. 1997, Pinsonneault et al. 1998)

ii) ${}^6\text{Li}$ abundances as a function of $[\text{Fe}/\text{H}]$ provide an additional test of theories for the production of the light elements Li, Be and B by interactions between fast nuclei and ambient ones (Ramaty et al. 1996, Yoshii et al. 1997, Fields & Olive 1999a,b, Vangioni-Flam et al. 1999).

iii) Information on depletion of ${}^6\text{Li}$ as a function of stellar mass and metallicity puts new constraints on stellar models in addition to those set by ${}^7\text{Li}$ depletion. This is so because the proton capture cross section of ${}^6\text{Li}$ is much larger than that of ${}^7\text{Li}$. Hence, at a given metallicity there will be a mass interval, where ${}^6\text{Li}$ but not ${}^7\text{Li}$ is being destroyed according to standard stellar models (Chaboyer 1994).

Altogether, ${}^6\text{Li}$ abundances may contribute to the study of such different fields as Big Bang nucleosynthesis, cosmic ray physics and stellar structure. It will, however, require a rather large data set of ${}^6\text{Li}$ abundances to get information in all these areas. The most metal-poor stars around the turnoff are of particular interest in connection with the determination of the primordial ${}^7\text{Li}$ abundance, whereas more metal-rich halo stars and disk stars are of interest for the study of the formation and astrophysics of the light elements.

Recent studies of ${}^6\text{Li}$ abundances have concentrated on halo stars. Following the first detection of ${}^6\text{Li}$ in HD 84937 by Smith et al. (1993) at a level corresponding to an isotopic ratio of ${}^6\text{Li}/{}^7\text{Li} \simeq 0.05$, Hobbs & Thorburn (1994, 1997) have confirmed the detection, and found upper limits of ${}^6\text{Li}/{}^7\text{Li}$ for 10 stars. More recently, Smith et al. (1998) report the probable detection of ${}^6\text{Li}$ in another

Send offprint requests to: P.E. Nissen

* Based on observations carried out at the European Southern Observatory, La Silla, Chile

halo star BD +26 3578 with about the same metal abundance, mass and evolutionary stage as HD 84937, and give tight upper limits of ${}^6\text{Li}/{}^7\text{Li}$ for 7 additional stars. Finally, Cayrel et al. (1999a) have observed the Li I line in HD 84937 with very high S/N and confirmed the presence of ${}^6\text{Li}$ with a high degree of confidence.

In the case of disk stars there has not been any systematic search for ${}^6\text{Li}$ since the studies of Andersen et al. (1984) and Maurice et al. (1984). In these papers an upper limit of ${}^6\text{Li}/{}^7\text{Li}$ of about 0.10 is set for about 10 disk stars ranging in metallicity from -1.0 to $+0.3$. The meteoritic ${}^6\text{Li}/{}^7\text{Li}$ ratio is close to 0.08 (Anders & Grevesse 1989) and the interstellar ratio is similar – possibly with significant variations (Lemoine et al. 1995). For metal-poor disk stars the ratio may be considerably higher than in the solar system. According to recent models for the galactic evolution of the light elements (Vangioni-Flam et al. 1999, Fields & Olive 1999a,b) the ${}^6\text{Li}/{}^7\text{Li}$ ratio reaches a maximum of about 0.3 at a metallicity of $[\text{Fe}/\text{H}] \simeq -0.5$. At higher metallicities the ratio decreases due to the production of ${}^7\text{Li}$ in AGB stars, novae and supernovae of type II by the ν -process (Matteucci et al. 1995, Woosley & Weaver 1995, Vangioni-Flam et al. 1996). Hence, it seems well justified to look for ${}^6\text{Li}$ in the metal-poor disk stars. Any detection will provide important constraints of the chemical evolutionary models, and with a large set of data it may also be possible to constrain the degree of ${}^6\text{Li}$ depletion as a function of stellar mass and metallicity.

In the present paper we present results for the ${}^6\text{Li}/{}^7\text{Li}$ ratio for five metal-poor disk stars ranging in metallicity from -0.8 to -0.6 . Very high S/N spectra of the Li I 6708 Å resonance line are presented in Sect. 3 and analyzed with model atmosphere techniques in Sect. 4. This has led to a rather clear detection of ${}^6\text{Li}$ in the two stars with the highest masses and tight upper limits for ${}^6\text{Li}$ in the other stars. The consequences of these results are discussed in Sect. 5.

2. Selection of stars

The program stars were selected from the large survey of nearby disk dwarfs by Edvardsson et al. (1993), which includes accurate values of atmospheric parameters, abundances, kinematics and ages of 189 main sequence stars distributed in metallicity from $[\text{Fe}/\text{H}] = -1.0$ to $+0.3$. As we wanted to avoid stars formed from interstellar gas greatly enriched in ${}^7\text{Li}$ from AGB stars or novae, the first condition for including a star was $[\text{Fe}/\text{H}] \lesssim -0.5$. Next, only stars with $T_{\text{eff}} \gtrsim 5900$ K were included in order to maximize the chance of survival of some ${}^6\text{Li}$. Finally, the program had to be limited to a few of the brightest stars in order to be able to reach the high S/N that is needed to determine the lithium isotope ratio from the profile of the 6707.8 Å Li I line.

The five stars observed are listed in Table 1. The effective temperature (derived from the $b - y$ color index),

Table 1. List of program stars including the visual magnitude m_V and atmospheric parameters adopted from Edvardsson et al. (1993)

HR	HD	m_V	T_{eff} [K]	$\log g$	$[\text{Fe}/\text{H}]$	ξ_{micro} [km s $^{-1}$]
2883	59984	5.93	5976	4.18	-0.75	1.7
3578	76932	5.80	5965	4.37	-0.82	1.4
8181	203608	4.23	6139	4.34	-0.67	1.6
		68284	7.77	5883	3.96	-0.59
			130551	7.16	6237	4.25
					-0.62	1.8

the logarithmic surface gravity, the iron abundance, and the microturbulence velocity, are taken from Edvardsson et al. (1993). Note, that none of the stars are significantly affected by interstellar reddening according to the color excesses derived from the H_{β} index and $b - y$. According to the kinematical parameters of the stars as given in Edvardsson et al. (1993) they belong to either the thick disk or the old thin disk. The α -elements, e.g. O and Mg, are somewhat enhanced in the stars, ranging from $[\alpha/\text{Fe}] \simeq 0.15$ in HR 8181, HD 68284 and HD 130551 to $[\alpha/\text{Fe}] \simeq 0.25$ in HR 2883 and HR 3578.

3. Observations and data reduction

The observations were carried out with the ESO Coudé Echelle Spectrometer (CES) in three different periods: October 22–27, 1992, June 6–8, 1993, and February 5–9, 1995. In Oct. 92 and Feb. 95 the CAT 1.4m telescope was applied, whereas in June 93 the 3.6m telescope was feeding the CES through a 35m long fiber and an image slicer (D’Odorico et al. 1989). On all occasions the detector was a front illuminated Ford Aerospace 2048 \times 2048 CCD with 15 μm pixels. The CES camera has a dispersion of 1.88 Å mm $^{-1}$ at 6700 Å providing a spectral coverage of about 58 Å and 0.0282 Å pixel $^{-1}$. Different settings for the central wavelength were applied on the various nights in order to avoid any signatures in the spectrum resulting from a possible improper flatfielding.

The main targets for the June 93 observations were some halo turnoff stars, for which the results have been presented by Smith et al. (1998) including a description of the reductions of the image slicer observations. The Oct. 92 and Feb. 95 observations have been reduced in much the same way. Subtraction of background, flat field correction and extraction of spectra were performed with standard tasks in IRAF. The wavelength calibration was based on 28 thorium lines well distributed over the wavelength region (6676 – 6734 Å). A second-order polynomial was adopted for the dispersion solution resulting in a typical rms deviation from the fit of 0.0015 Å. Furthermore, the FWHM of the thorium lines were measured and found to vary by less than 4% along the spectrum. This near-constancy of the instrument profile is important in

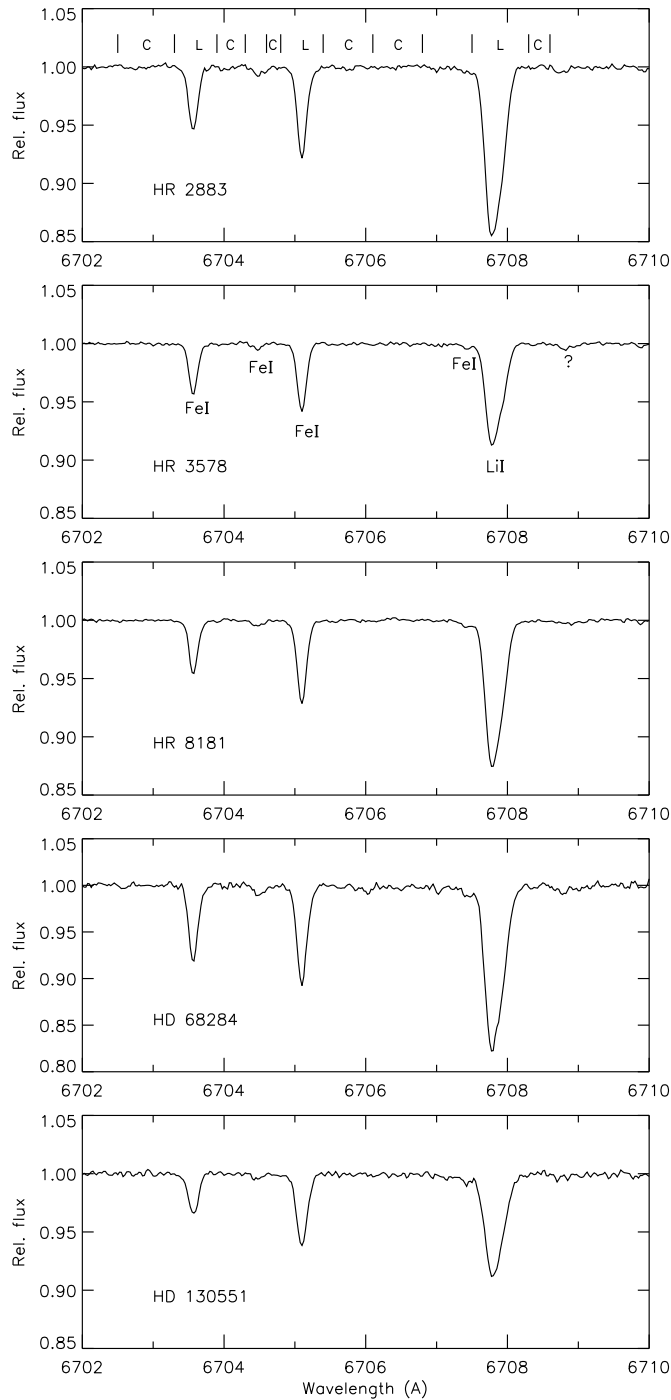


Fig. 1. The observed spectra in the 6702 – 6710 Å region. Spectral windows used in defining the continuum and in the χ^2 analysis of the lines are marked with C and L, respectively. Line identifications are shown for HR 3578

connection with the determination of instrumental and stellar line broadening from FeI lines near the LiI line. For the Oct. 92 and Feb. 95 observations the FWHM of the Th lines corresponds to a resolution of $R = 105\,000$,

Table 2. Number of observations and exposure times for the program stars

ID	Oct. 92	June 93	Feb. 95
	CAT 1.4m	3.6m	CAT 1.4m
HR 2883	4 × 40 min		
HR 3578	3 × 60 min	2 × 25 min	2 × 45 min
HR 8181	4 × 30 min	2 × 10 min	
HD 68284			8 × 60 min
HD 130551			6 × 50 min

whereas the June 93 image slicer spectra have a resolution of $R = 115\,000$. Finally, the spectra were normalized to an approximate level of 1 by fitting a fifth-order cubic spline function to the continuum, and corrected for the radial velocity shift using the accurate wavelengths (6703.567 and 6705.102 Å) given by Nave et al. (1995) for the two FeI lines close to the the Li line.

Table 2 lists the the number of observations and exposure times as distributed over the three periods. Note, that HR 3578 has been observed in all three periods and HR 8181 in two of them. The individual spectra show excellent agreement and have therefore been co-added to obtain the final spectra shown in Fig. 1 for the 6702 – 6710 Å region. These are the spectra used for the determination of the ${}^6\text{Li}/{}^7\text{Li}$ ratio, but in the case of HR 3578 we have also derived the ratio separately for each observing period in order to check for possible systematic differences.

4. The isotope ratio ${}^6\text{Li}/{}^7\text{Li}$

4.1. The center-of-gravity wavelength of the LiI line

As discussed by e.g. Smith et al. (1998) the ${}^6\text{Li}/{}^7\text{Li}$ ratio can be determined by two methods: From the center-of-gravity (cog) of the LiI 6708 Å line or from a detailed model atmosphere synthesis of the profile. The isotopic shift of the ${}^6\text{Li}$ doublet is +0.158 Å relative to the ${}^7\text{Li}$ doublet. Addition of ${}^6\text{Li}$ therefore shifts the LiI line to longer wavelengths and increases the FWHM. The cog-method relies in principle on a very simple and straightforward measurement, but its accuracy is limited by possible errors in the laboratory wavelengths of the lithium line and the reference lines needed to correct for the radial velocity shift of the star. The errors in the laboratory wavelengths are typically $\pm 2\text{ m}\text{\AA}$. Differences in convective blueshifts may well be of the same order of size (Dravins 1987). To this should be added the uncertainty in measuring the cog- λ for an asymmetric lithium line, which is slightly blended by a weak FeI line in the blue wing. According to our experience the cog- λ will be uncertain by about $\pm 5\text{ m}\text{\AA}$. This translates to a one-sigma error of ± 0.03 in ${}^6\text{Li}/{}^7\text{Li}$, which is inferior to what may be obtained with the profile method. Hence, only the profile method will be used, and the wavelength of the LiI line will be considered as a

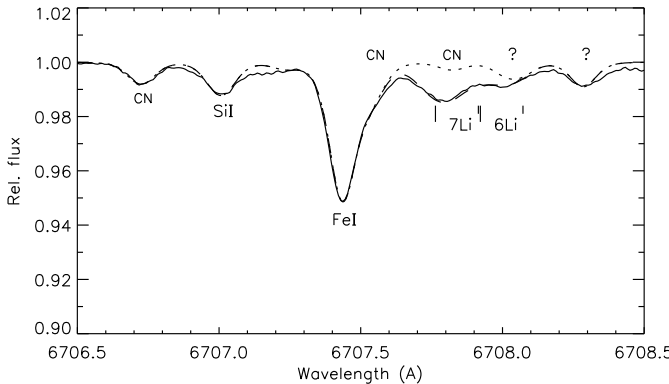


Fig. 2. The solar flux spectrum around the Li I line. The full drawn line is the observed spectrum from the Solar Flux Atlas of Kurucz et al. (1984). The dashed line is the synthetic spectrum computed for the model atmosphere of the Sun. The dotted line is the synthetic spectrum without the Li I line

free parameter in the comparison between synthetic and observed profiles.

4.2. Synthetic spectra

The synthetic spectra have been obtained with the Uppsala Synthetic Spectrum Package, which computes the flux in a given wavelength region for an OSMARC model atmosphere of the star (Edvardsson et al. 1993). LTE is assumed and thermal and microturbulent line broadening as well as pressure broadening is included. The resulting spectrum is folded with a line broadening function that can be either Gaussian, radial-tangential (Gray 1978), rotational (Gray 1992) or any combination of these functions. As a check, one star (HD 68284) has also been analyzed with a Kurucz ATLAS9 model atmosphere and the SYNTHE code (Kurucz 1993).

Wavelengths and *gf*-values for the ^6Li and ^7Li components of the Li I doublet are taken from Table 3 of Smith et al. (1998). As discussed by Smith et al. these values are not a source of significant errors in connection with determinations of the isotopic abundances of Li.

In the case of halo turnoff stars with $[\text{Fe}/\text{H}] < -1.5$ there is no significant blending of the Li I line by other lines, but already at $[\text{Fe}/\text{H}] \simeq -1.0$ one has to worry about contributions from other absorption lines. To get more detailed information about line blending we therefore started by synthesizing the solar spectrum, which is well suited for studying this problem because of the weakness of the Li I line. Fig. 2 shows the solar flux spectrum from the atlas of Kurucz et al. (1984) compared to a synthetic spectrum based on the OSMARC solar model and a list of CN and metal lines from Müller et al. (1975), who obtained $\log \epsilon(\text{Li}) = 1.0$ and $^6\text{Li}/^7\text{Li} \simeq 0.0$ from a synthesis analysis of the solar Li I feature. We adopted these values and adjusted the *gf*-values of the other lines to get the

best possible fit of the synthetic spectrum (broadened by a radial-tangential function with a FWHM = 2.5 km s^{-1}) to the Solar Flux Atlas. As seen from Fig. 2 the fit is quite satisfactory. The main problem is the two unidentified weak lines at 6708.02 and 6708.28 Å , which have equivalent widths of 0.6 and 1.1 mÅ , respectively. The first line has nearly the same wavelength as the weak component of the ^6Li doublet and therefore makes the determination of $^6\text{Li}/^7\text{Li}$ very tricky for solar-type metallicities, whereas the unidentified line at 6708.28 Å is further away and only affects the determination of the lithium isotope ratio marginally.

Assuming that the two unidentified lines are neutral metal lines they will have equivalent widths less than 0.15 and 0.3 mÅ , respectively, in solar-type stars with $[\text{Fe}/\text{H}] \lesssim -0.6$. This is too small to have any significant effect on the determination of the lithium isotope ratio. If the lines are ionized metal lines they will be somewhat stronger and affect the determination of $^6\text{Li}/^7\text{Li}$ marginally at the 1% level. The probability for lines in solar-type spectra being from ionized metals instead of neutral is, however, small, and we have therefore chosen to exclude the two unidentified lines from our model atmosphere synthesis of the metal-poor disk stars.

The CN lines seen in Fig. 2 play no rôle in the spectra of the program stars mainly because both C and N scales almost linearly with Fe and partly because the stars have somewhat higher effective temperatures than the Sun. Hence, there is no reason to include these lines. The only line that has a significant effect on the synthesis of the lithium line is the Fe I line at 6707.43 Å . This line was included with the *gf*-value derived from the fit to the solar spectrum.

As discussed in Sect. 4.3 the Fe I lines at 6703.6 and 6705.1 Å have been used to determine the instrumental and stellar atmospheric line broadening. The two lines are blended by several faint CN lines in the solar spectrum as seen from Fig. 2 of Brault & Müller (1975), but the synthesis of the solar and stellar spectra shows that these lines disappear beyond detection in the program stars. The same technique has been used to define a number of spectral windows practically free of lines in the program stars. These regions are marked by ‘C’ in Fig. 1, and are used to set the continuum and to estimate the S/N in connection with the chi-square analysis of the lines.

4.3. χ^2 analysis

The synthetic spectra were computed for model atmospheres with the parameters given in Table 1. Line broadening due to macroturbulence and rotation was determined from the two Fe I lines at 6703.6 and 6705.1 Å with $\chi_{exc} = 2.76$ and 4.61 eV , respectively. The synthetic spectrum was first folded with a Gaussian function representing the instrumental profile and then with either a Gaussian, a radial-tangential or a rotational profile. Various

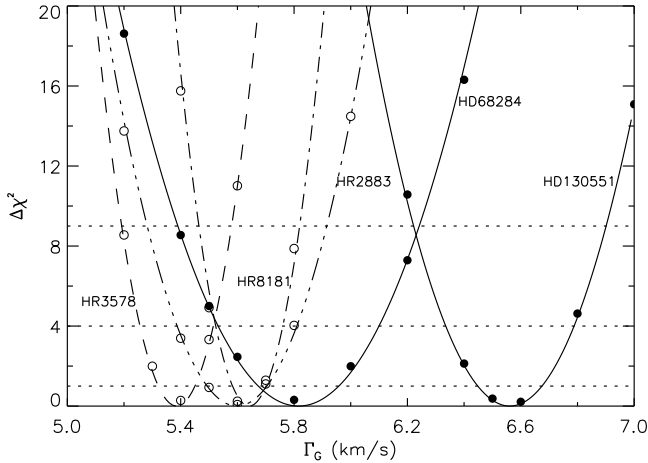


Fig. 3. Variation of the χ^2 of the fit to the Fe I 6705.1 Å line as a function of the FWHM of the Gaussian broadening function

combinations of these profiles was also tried, but in no cases the fit to the iron lines was better than that obtained with a Gaussian function. The final analysis was therefore carried out with a single Gaussian representing the combined effect of instrumental and stellar atmospheric broadening.

The FWHM of the Gaussian broadening profile, Γ_G , has been determined with the following procedure. First the continuum is set from the two windows on each side of a Fe I line and at the same time the standard deviation, $\sigma = (S/N)^{-1}$ of the spectrum is estimated. Then the chi-square function is computed:

$$\chi^2 = \Sigma \left[\frac{(O_i - S_i)^2}{\sigma^2} \right] \quad (1)$$

where O_i is the observed spectral point and S_i is the synthesis. The summation is performed over the spectral interval marked by 'L' in Fig. 1 corresponding to $N = 25$ datapoints. In addition to Γ_G , the equivalent width and the exact wavelength of the Fe I line are considered as free parameters. Γ_G is varied in steps of 0.1 or 0.2 km s^{-1} and the other two parameters are optimized for each value of Γ_G to find the lowest χ^2 . This results in a parabolic variation of χ^2 as shown in Fig. 3. The most probable value of Γ_G corresponds to the minimum of χ^2 , and $\Delta\chi^2 = 1, 4$ and 9 correspond to the 1-, 2-, and 3- σ confidence limits of determining Γ_G alone (Bevington & Robinson 1992).

Table 3 summarizes the results of the χ^2 fitting of the two Fe I lines. Note, that the reduced chi-square ($\chi^2_{\text{red}} = \chi^2/\nu$, where $\nu = 22$ is the number of degrees of freedom in the fit) is satisfactorily close to 1. Furthermore, the values of Γ_G from the two Fe I lines agree rather well, although there is a tendency that the 6705.1 Å line gives slightly higher values of Γ_G than the 6703.6 Å line.

Adopting a weighted average of Γ_G from Table 3 the lithium isotope ratio is determined from a χ^2 analysis of the fit between the computed and observed profile of

Table 3. Results from the χ^2 analysis of the Fe I lines at 6703.6 and 6705.1 Å. Γ_G (6703) and Γ_G (6705) are the FWHM of the Gaussian broadening function (instrumental + rotation + macroturbulence) applied to the synthetic lines. The errors given are the formal one-sigma errors resulting from the χ^2 analysis

ID	S/N	Γ_G (6703) [km s^{-1}]	χ^2_{red}	Γ_G (6705) [km s^{-1}]	χ^2_{red}
HR 2883	700	5.70 ± 0.17	0.78	5.60 ± 0.11	1.36
HR 3578	1250	5.35 ± 0.09	1.07	5.40 ± 0.06	1.05
HR 8181	1370	5.25 ± 0.08	1.17	5.65 ± 0.05	1.22
HD 68284	400	5.40 ± 0.20	0.96	5.80 ± 0.14	0.93
HD 130551	830	6.30 ± 0.15	1.05	6.55 ± 0.10	0.96

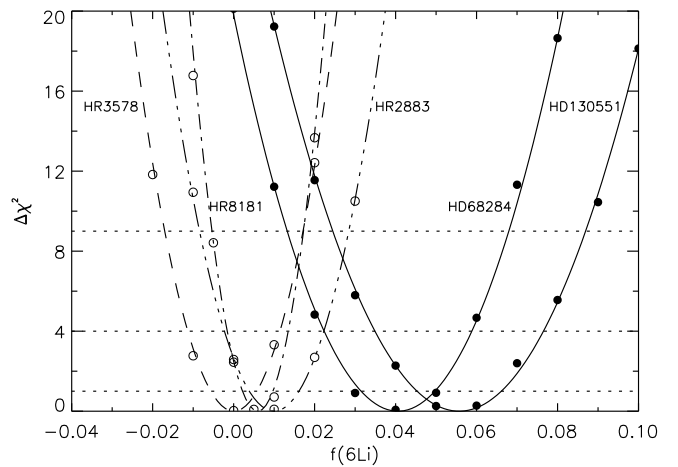


Fig. 4. Variation of the χ^2 of the fit to the Li I 6707.8 Å line as a function of the relative abundance of ${}^6\text{Li}$

the Li I line. The free parameters in the fit are the total lithium abundance of the star, $\log(\epsilon(\text{Li}))$, and the ${}^6\text{Li}$ fraction, $f({}^6\text{Li}) = N({}^6\text{Li})/N(\text{Li})$. Furthermore, a wavelength shift, $\Delta\lambda$, of the Li line relative to the wavelengths given in Table 3 of Smith et al. (1998) is allowed. The continuum and the S/N are determined from the two adjacent windows shown in Fig. 1 (resulting in nearly the same S/N values as given in Table 3) and the χ^2 analysis is carried out over the region marked by 'L', i.e. over $N=33$ data-points. Note, that the weak Fe I line at 6707.43 Å has only a small effect on the flux in this line region.

The relative ${}^6\text{Li}$ abundance is varied in steps of 0.01 and the other two parameters, $\log(\epsilon(\text{Li}))$ and $\Delta\lambda$, are optimized for each value of $f({}^6\text{Li})$ to find the lowest χ^2 . In order to study the behaviour of the χ^2 function around $f({}^6\text{Li}) = 0.00$ 'negative' values of $f({}^6\text{Li})$ have been simulated by subtracting the line absorption coefficient due to ${}^6\text{Li}$ from the continuous absorption coefficient instead of adding it.

The results of the χ^2 analysis are summarized in Table 4 and the variation of χ^2 with $f({}^6\text{Li})$ is shown in Fig. 4. As seen, the three 'HR' stars have $f({}^6\text{Li})$ close to zero,

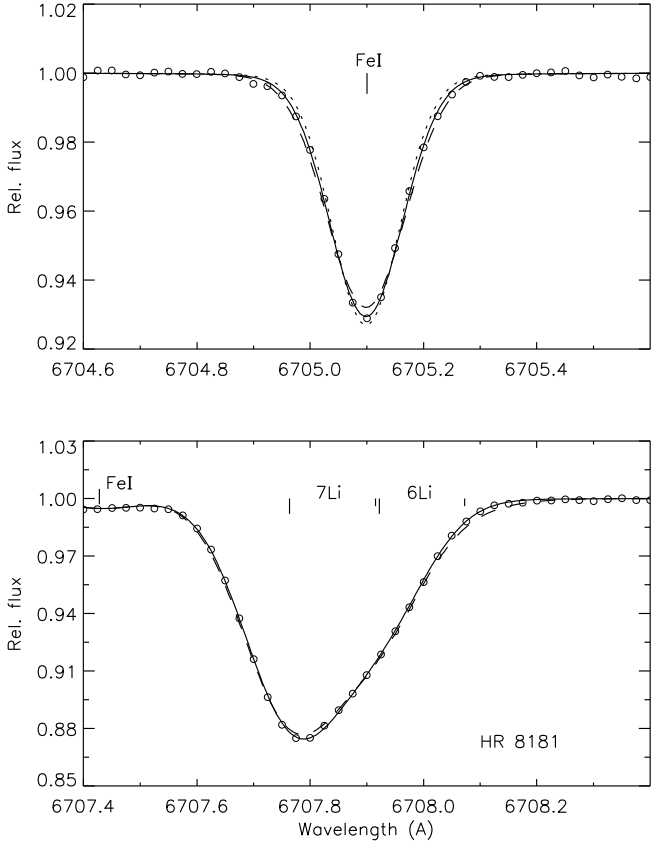


Fig. 5. The model atmosphere synthesis of the Fe I 6705.1 Å and the Li I 6707.8 Å line in the spectrum of HR 8181. The datapoints are shown with open circles. In the upper figure the full drawn line corresponds to a Gaussian broadening parameter of $\Gamma_G = 5.6 \text{ km s}^{-1}$, whereas the dotted and dashed lines correspond to $\Gamma_G = 5.0$ and 6.2 km s^{-1} , respectively. In the lower figure $\Gamma_G = 5.5 \text{ km s}^{-1}$ has been applied. The full drawn line corresponds to $f(^6\text{Li}) = 0.0$ and the dashed line to $f(^6\text{Li}) = 0.05$. Note, that when Γ_G and $f(^6\text{Li})$ are varied the other free parameters in the fits, the wavelengths and the equivalent widths of the lines, have been optimized to get the best possible fits

whereas ^6Li has been detected in the two ‘HD’ stars at a high confidence level. As a further illustration of this result Figs. 5 and 6 show the fits to the Fe I and the Li I for two stars – one with $f(^6\text{Li}) \simeq 0.0$ and the other one with $f(^6\text{Li}) \simeq 0.06$ – and Fig. 7 shows a plot of the residuals in the observations after subtracting the ^7Li and Fe I part of the synthesis. Although there is a disturbing periodic noise in the residuals with an amplitude of 0.1 to 0.2% in addition to the shot noise (the reason for which remains unexplained) a clear residual absorption at the wavelength of the ^6Li doublet is seen in the spectra of HD 68284 and HD 130551. Note, that although the S/N of the spectrum

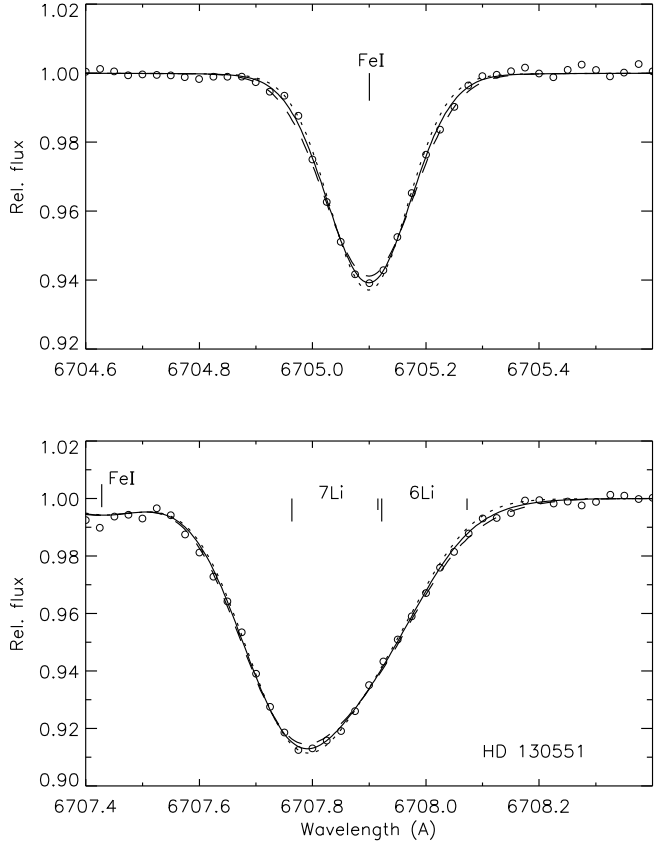


Fig. 6. Same as Fig. 4 for HD 130551. In the upper figure the full drawn line corresponds to a Gaussian broadening parameter of $\Gamma_G = 6.6 \text{ km s}^{-1}$, and the dotted and dashed lines to $\Gamma_G = 6.0$ and 7.2 km s^{-1} , respectively. In the lower figure $\Gamma_G = 6.6 \text{ km s}^{-1}$ has been applied. Here the full drawn line corresponds to $f(^6\text{Li}) = 0.06$ and the dotted and dashed lines to $f(^6\text{Li}) = 0.00$ and 0.10 , respectively

of HD 68284 is inferior to that of HD 130551, the error of $f(^6\text{Li})$ is nearly the same for the two stars, because the Li line is about a factor of two stronger in the spectrum of HD 68284 than in the case of HD 130551.

In order to check that there are no significant systematic differences between the results obtained for the three observing periods the individual spectra of HR 3578 were analyzed separately including the determination of Γ_G . The χ^2 analysis gave the following values: $f(^6\text{Li}) = -0.018 \pm 0.012$, $+0.008 \pm 0.010$, and -0.006 ± 0.014 for the Oct. 92, June 93 and Feb. 95 spectra. Within the errors these values agree satisfactorily with the value ($f(^6\text{Li}) = 0.000 \pm 0.006$) derived for the averaged spectrum.

Table 4. Results from the χ^2 analysis of the Li I line. Γ_G is the weighted average of the FWHM of the Gaussian broadening function determined from the Fe I lines at 6703.6 and 6705.1 Å (Table 3). $\log\epsilon(\text{Li})$ is the total Li abundance and $f(^6\text{Li})$ is the relative abundance of ^6Li . The errors given are the formal one-sigma errors resulting from the χ^2 analysis. The last column gives the reduced chi-square of the fit

ID	Γ_G [km s^{-1}]	$\log\epsilon(\text{Li})$	$f(^6\text{Li})$	χ^2_{red}
HR 2883	5.7	2.34	$0.010 \pm .007$	0.99
HR 3578	5.4	2.05	$0.000 \pm .006$	1.03
HR 8181	5.5	2.38	$0.004 \pm .004$	0.89
HD 68284	5.6	2.35	$0.041 \pm .010$	1.09
HD 130551	6.5	2.30	$0.056 \pm .011$	1.22

4.4. Systematic errors of $^6\text{Li}/^7\text{Li}$

The errors of $f(^6\text{Li})$ given in Table 4 are purely statistical. In addition we must consider possible systematic errors resulting from approximations in the model atmospheres and the spectrum synthesis of the Fe I and Li I lines.

First we note that the exact values of the atmospheric parameters of the models are not critical for the lithium isotope ratio derived. An increase of T_{eff} with +100 K changes $\log\epsilon(\text{Li})$ with +0.07 dex but $f(^6\text{Li})$ is practically unchanged. Changes in the gravity within reasonable limits have completely negligible effects. A decrease of the microturbulence by say 0.4 km s^{-1} is compensated by a slight increase of Γ_G and the change of $f(^6\text{Li})$ is less than 0.003. A more significant, but still rather small change, results from the use of Kurucz's model atmospheres (Kurucz 1993) instead of the OSMARC models. As an example a model atmosphere with the parameters of HD 68284 was interpolated between the closest models in the Kurucz ATLAS9 grid (re-computed with the "approximate" overshooting option switched off) and the SYNTHE code was used to compute profiles of the Fe I and Li I lines. This resulted in an increase of Γ_G from 5.6 to 5.9 km s^{-1} and a change of $f(^6\text{Li})$ from 0.041 to 0.033. Hence, the class of plane-parallel model atmospheres adopted has some effect on the value of the lithium isotope ratio derived, but not large enough to question the detection of ^6Li in HD 68284 and HD 130551.

A more critical problem is whether classical plane-parallel model atmospheres are good enough for a determination of $f(^6\text{Li})$ with an accuracy of say ± 0.01 . It is well known that convective motions in real atmospheres produce slightly asymmetric line profiles, i.e. curved bisectors with a shape that depends on the depth of line formation (e.g. Dravins 1987). The question is therefore if the atmospheric velocity broadening determined from the two Fe I lines is also valid for the Li I line. Due to the low excitation potential of the lithium resonance line it

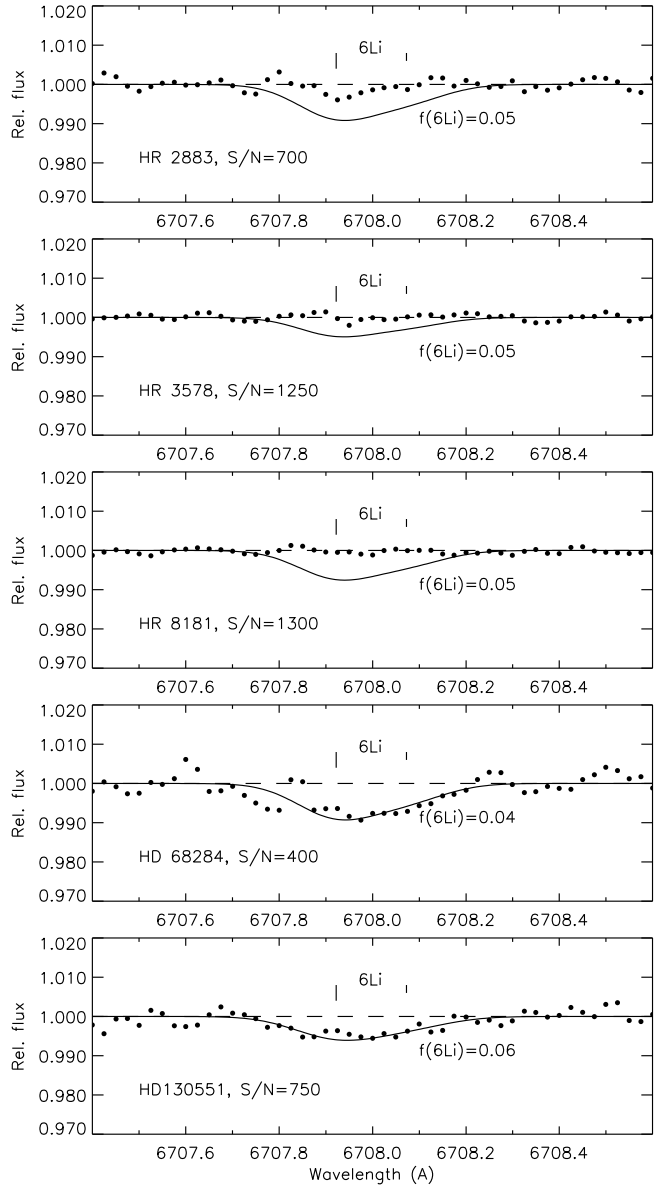


Fig. 7. The residuals of the observations after subtraction of the ^7Li and Fe I 6707.43 Å part of the synthesis of the Li I line. For comparison the synthesis of the ^6Li doublet is shown with a full drawn line

is probably formed somewhat higher in the atmosphere than the iron lines. In the case of HD 130551 a drastic increase of Γ_G to 7.5 km s^{-1} instead of the value derived from the Fe I lines, (6.5 km s^{-1}) decreases $f(^6\text{Li})$ to about zero. One could also imagine that the Li I line in HD 68284 and HD 130551 has a red asymmetry that mimics the ^6Li doublet although no such asymmetry is seen in the profiles of the Fe I lines. However, such possible effects have to occur for HD 68284 and HD 130551 only, because we can not allow a reduction of $f(^6\text{Li})$ for the other three stars

Table 5. Radial velocities of the stars as derived from the accurate wavelengths of the Fe I lines (6703.567 and 6705.102 Å) measured by Nave et al. (1995). The wavelength shifts given are obtained from the χ^2 fits of the synthetic spectra to the individual lines

ID	RV [km s ⁻¹]	$\Delta\lambda(6703)$ [mÅ]	$\Delta\lambda(6705)$ [mÅ]	$\Delta\lambda(\text{Li I})$ [mÅ]
HR 2883	+54.8	-0.1	+0.0	4.3
HR 3578	+119.4	+1.3	-1.4	9.1
HR 8181	-28.8	+2.6	-2.5	6.7
HD 68284	+62.8	+1.3	-1.4	1.8
HD 130551	+33.7	+1.4	-1.4	0.1

which have $f(^6\text{Li}) \simeq 0.00$, when the atmospheric velocity broadening of the Fe I lines is adopted.

As seen from Table 1 there are indeed significant differences in the atmospheric parameters of the two ‘HD’ stars and the three ‘HR’ stars that could induce some differential effects in the broadening of the Fe I and Li I lines. HD 68284 has a lower gravity and HD 130551 has a higher T_{eff} than the other three stars. A hint that there may be systematic differences in the convective pattern between the two groups of stars comes from the small changes of the laboratory wavelengths needed to optimize the χ^2 fit of the Fe I and Li I lines (see Table 5). The apparent heliocentric radial velocities (including gravitational redshift and convective blueshift) is determined from the two Fe I lines. Hence, the sum of the wavelength shifts for these two lines is zero by definition. As seen, the wavelength shift of the Li I line is always positive. The average value is 4.4 mÅ (corresponding to a redshift of 0.20 km s⁻¹ of the Li I line relative to the Fe I lines) and the rms scatter is 3.4 mÅ. This is more than the expected error of the laboratory wavelengths. In particular, we note that the redshift for HD 68284 and HD 130551 are lower than the redshift for the other three stars. Although this could be accidental, it is a warning that there may be differential effects in the convective line broadening. Clearly, this problem should be further studied by applying recently constructed inhomogeneous 3D hydrodynamical model atmospheres (Asplund et al. 1999) in the analysis of the Li I line.

5. Discussion

5.1. Stellar masses

According to standard stellar models the depletion of lithium is a strong function of stellar mass (Pinsonneault et al. 1992). Hence, it is of considerable interest to determine the masses of the stars. This can be done by comparing T_{eff} and absolute magnitude, M_V , with mass tracks from stellar evolution calculations.

Using the apparent magnitudes given in Table 1 and parallaxes from The Hipparcos and Tycho Catalogues

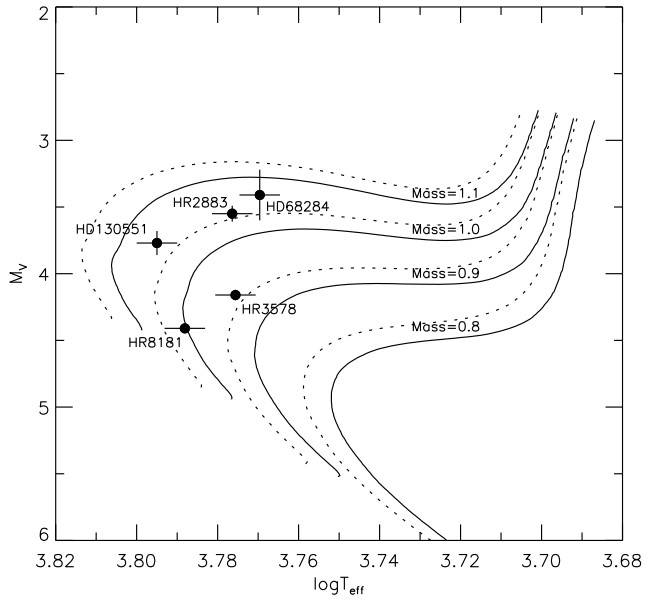


Fig. 8. Position of the stars in the $\log T_{\text{eff}} - M_V$ diagram compared with mass tracks from VandenBerg et al. (1999). Masses are given in units of the solar mass. The full drawn lines refer to $[\text{Fe}/\text{H}] = -0.61$ (equal to the metallicity of HD 68284 and HD 130551) and the dotted lines to $[\text{Fe}/\text{H}] = -0.71$ (approximately equal to $[\text{Fe}/\text{H}]$ of the other stars). Both sets of tracks have $[\alpha/\text{Fe}] = 0.3$. The error bars in the x-direction correspond to $\sigma(T_{\text{eff}}) = \pm 70$ K and those in the y-direction to the errors of the Hipparcos parallaxes

Table 6. Absolute magnitudes computed from m_V and Hipparcos parallaxes and masses and ages derived from stellar evolutionary tracks and isochrones of VandenBerg et al. (1999)

ID	M_V	$\mathcal{M}/\mathcal{M}_{\odot}$	Age [Gyr]
HR 2883	$3.55 \pm .06$	$1.02 \pm .02$	7.6 ± 0.6
HR 3578	$4.16 \pm .04$	$0.88 \pm .02$	11.7 ± 1.2
HR 8181	$4.41 \pm .01$	$0.96 \pm .02$	6.3 ± 2.0
HD 68284	$3.41 \pm .19$	$1.07 \pm .04$	6.8 ± 1.4
HD 130551	$3.77 \pm .09$	$1.06 \pm .02$	6.0 ± 0.9

(ESA 1997) the absolute magnitudes are calculated (Table 6), and the stars are plotted in the $\log T_{\text{eff}} - M_V$ diagram (Fig. 8). The mass tracks shown are from the new, α -element enhanced, evolutionary models of VandenBerg et al. (1999). Interpolation between the mass tracks (taking into account their dependence on $[\text{Fe}/\text{H}]$) leads to the masses given in Table 6, and from the corresponding isochrones the stellar ages given are obtained.

The errors of the masses and ages given in Table 6 are standard errors corresponding to the adopted errors of T_{eff} and M_V . Additional errors may be present due to inadequate stellar models and uncertainties in the cal-

ibration of T_{eff} and the bolometric correction. Such errors are, however, more systematic and are expected to affect all stars with about the same amount. Hence, we conclude from Table 6 that the two stars for which ${}^6\text{Li}$ has been detected (HD 68284 and HD 130551) have significantly higher masses than the three stars with no ${}^6\text{Li}$ present in their atmospheres. This makes sense, because the depth of the convection zone of a star on the main sequence decreases rapidly as a function of increasing mass. Hence, according to standard stellar models without mixing, the depletion of ${}^6\text{Li}$ is less severe in the more massive stars. In this connection we note that although HD 68284 is already on the subgiant branch and the coolest of the stars, it has spent most of its life as a main sequence star at $T_{\text{eff}} \simeq 6300$ K.

5.2. Galactic evolution and stellar depletion of ${}^6\text{Li}$

Interpretation of the novel result of this paper - the detection and quantitative measurement of the ${}^6\text{Li}$ abundance in two old metal-poor disk stars - is contingent on two factors: (i) the expected evolution of the interstellar ${}^6\text{Li}$ abundance with metallicity, and (ii) the depletion of the stellar ${}^6\text{Li}$ abundance by the convective mixing that occurs in the pre-main sequence phase, and the additional depletion occurring on the main sequence.

As is all too well known, prediction of Li depletion by main sequence stars and subgiants is an imprecise art. Standard models by Pinsonneault et al. (1992) predict loss of lithium in the pre-main sequence phase and no subsequent loss for stars of the mass of our quintet. Depletions for masses of up to $0.85M_{\odot}$ and metallicities corresponding to $[\text{Fe}/\text{H}] = -2.6$ and -1.6 are computed by Pinsonneault et al. For their $0.85M_{\odot}$ model, the predicted ${}^7\text{Li}$ -depletions are negligible and the ${}^6\text{Li}$ -depletions are 0.3 dex at $[\text{Fe}/\text{H}] = -1.6$ and by extrapolation less than 0.05 dex at $[\text{Fe}/\text{H}] = -2.6$. Extrapolation to $[\text{Fe}/\text{H}] \simeq -0.7$ is uncertain but these depletions decrease with increasing mass such that our stars might be anticipated to have lost little, if any, ${}^6\text{Li}$. Cayrel et al. (1999b) report calculations that essentially confirm the above pre-main sequence depletions but predict a substantial continuing depletion of ${}^6\text{Li}$ on the main sequence. At $M = 0.85M_{\odot}$ and $[\text{Fe}/\text{H}] = -1.5$, a total ${}^6\text{Li}$ depletion of about 0.7 dex is predicted in contrast to the 0.3 dex expected by Pinsonneault et al. Consideration of non-standard physics, especially rotationally-induced mixing will result in likely larger and as yet more uncertain depletions - see, for example, the state of the art calculations by Pinsonneault et al. In summary, depletion of ${}^6\text{Li}$ is to be expected but, at present, the magnitude of this depletion is uncertain with even standard calculations unavailable for the mass and metallicity of our old disk stars.

Encouraged by recent observations of ${}^6\text{Li}$, Be, and B several predictions about the galactic chemical evolution of Li, Be, and B have appeared. Behind such predictions

are assumptions about the nucleosynthetic processes of Li, Be, and B manufacture that demand assumptions about the early Galaxy, especially about the cosmic rays that permeated the halo and then the disk. Qualitatively, the key nucleosynthetic processes are known: (i) the Big Bang provided only the ${}^7\text{Li}$ (in addition to H, ${}^2\text{H}$, ${}^3\text{He}$, and ${}^4\text{He}$) that is widely considered to account for the observed Li abundance of the warm halo stars, the so-called Spite plateau; (ii) interactions between standard GCR and ISM and/or interactions between fast C,N,O nuclei from superbubbles with H or He in the ISM provide Li, Be, and B by spallation processes (e.g., $\text{O} + \text{p} \rightarrow \text{Be}$) and Li through the fusion process $\alpha + \alpha \rightarrow {}^6\text{Li}$ and ${}^7\text{Li}$; (iii) neutrino-induced spallation processes in Type II supernovae that may provide ${}^7\text{Li}$ and ${}^{11}\text{B}$.

A key facet of this suite of processes is that beryllium with ${}^9\text{Be}$ as the single stable isotope is produced solely by spallation of C,N,O in flight or at rest. Hence, observed beryllium abundances may be used to calibrate the yields of cosmic ray spallation. This is especially useful now that there are extensive measurements of the Be abundance in disk and halo dwarf stars. The relative yields of light nuclides, for example ${}^6\text{Li}$ to ${}^9\text{Be}$, are essentially independent of the cosmic ray spectrum unless there is a large excess of low energy cosmic rays ($E < 30$ MeV nucleon $^{-1}$) with respect to higher energy particles. This happy circumstance arises because above the similar threshold energies for the different processes (e.g., ${}^9\text{Be}$ from $\text{p} + \text{O}$ and ${}^{10}\text{B}$ also from $\text{p} + \text{O}$), the spallation cross-sections are almost energy independent. That ratios of yields are independent of the form of the (high) energy spectrum was well illustrated by Ramaty et al. (1996). At energies around the threshold energies for the various processes, the relative yields are energy and composition dependent. Moreover, Li production occurs also through $\alpha + \alpha$ fusion reactions that do not synthesize Be and B.

The B/Be ratio of halo stars is consistent within measurement uncertainty with production by spallation: Duncan et al. (1997) estimated $\text{B}/\text{Be} = 15 \pm 3$ and García López et al. (1998) from a similar dataset of HST spectra found $\text{B}/\text{Be} = 17 \pm 10$. Relativistic cosmic rays and the suite of (p,α) on (C,N,O) processes are predicted to give $\text{B}/\text{Be} \simeq 14$ - see Ramaty et al. (1996) for predicted B/Be ratios as a function of cosmic ray energy and composition. It has long been known that spallation by relativistic cosmic rays is inadequate to account for the solar system's ${}^{11}\text{B}/{}^{10}\text{B}$ ratio which at 4.05 exceeds the prediction of about 2.5. Low energy spallation or a contribution from Type II supernovae are needed to resolve this discrepancy.

These uncertainties aside, the Be observations are a reasonably firm basis from which to predict the ${}^6\text{Li}$ abundances provided by spallation. Smith et al. (1998) discussed the prediction of ${}^6\text{Li}$ abundances from observed Be abundances - see the long-dashed line in Fig. 9, where beryllium abundances are taken from Gilmore et al. (1992)

and Boesgaard et al. (1999b). Predicted ${}^6\text{Li}$ abundances are about a factor of 10 less than the observed ${}^6\text{Li}$ abundances in the halo stars HD 84937 and BD +26°3578 but exceed the ${}^6\text{Li}$ abundances reported here for the disk stars HD 68284 and HD 130551 by about a factor of 3. Since ${}^6\text{Li}$ has almost certainly been depleted during pre-main sequence evolution and possibly during residence on the main sequence, the initial or interstellar ${}^6\text{Li}$ abundance for the halo stars was higher than now observed. The required additional ${}^6\text{Li}$ is probably primarily a product of cosmic ray $\alpha + \alpha$ fusion production.

Predictions of the growth of ${}^6\text{Li}$ in the Galaxy made recently by Fields & Olive (1999a,b), Vangioni-Flam et al. (1999) and Yoshii et al. (1997) are shown in Fig. 9. These call on the same production processes but in different proportions.

Fields & Olive discuss what they term the standard picture of galactic cosmic ray nucleosynthesis in a model galaxy. The key assumptions are that the cosmic rays always had the composition of the ambient interstellar gas (i.e., they were very CNO-poor early in the life of the Galaxy), the energy spectrum of the cosmic rays was that measured for contemporary cosmic rays in the solar neighborhood (i.e., relativistic energies are dominant), and the cosmic ray flux has been proportional to the local supernova rate, and scaled so that solar abundances of ${}^6\text{Li}$, B, and ${}^{10}\text{B}$ are reproduced. These assumptions with a simple chemical evolution code (Fields & Olive report results for the canonical closed box) lead to the predicted run of the ${}^6\text{Li}$ abundances with $[\text{Fe}/\text{H}]$ where iron is a product of stellar nucleosynthesis with yields from Woosley & Weaver (1995) and a standard initial mass function. The key novel ingredient in the otherwise familiar calculation is the incorporation of recent measurements of the oxygen abundance in halo stars that indicate $[\text{O}/\text{Fe}]$ increasing with decreasing $[\text{Fe}/\text{H}]$ (Israelian et al. 1998; Boesgaard et al. 1999a). A higher O abundance increases the yields of spallation products. (A ‘fudge’ is needed as the O/Fe from these recent observations is considerably higher than predicted for Type II supernovae). The predicted ${}^6\text{Li}$ vs $[\text{Fe}/\text{H}]$ relation is shown by the dotted line in Fig. 9. A large part of the increase in the ${}^6\text{Li}$ prediction at low $[\text{Fe}/\text{H}]$ over the simple expectation from spallation is due to the inclusion of the $\alpha + \alpha$ fusion reactions but the use of the observed O abundances through the associated contribution from $\text{p} + \text{O}$ spallation appears necessary to match the observed ${}^6\text{Li}$ abundances of the halo stars. Fields & Olive adjust their model to reproduce the solar ${}^6\text{Li}$ which also accounts well for the Be and B abundances of the sun, disk and halo stars.

Vangioni-Flam et al. (1999) incorporate a different mix of the light element producing processes into their chemical evolution model. In particular, they invoke low energy nuclei that they associate with the acceleration of supernovae ejecta in the superbubbles created collectively by winds from the massive stars in OB associations. (‘Low

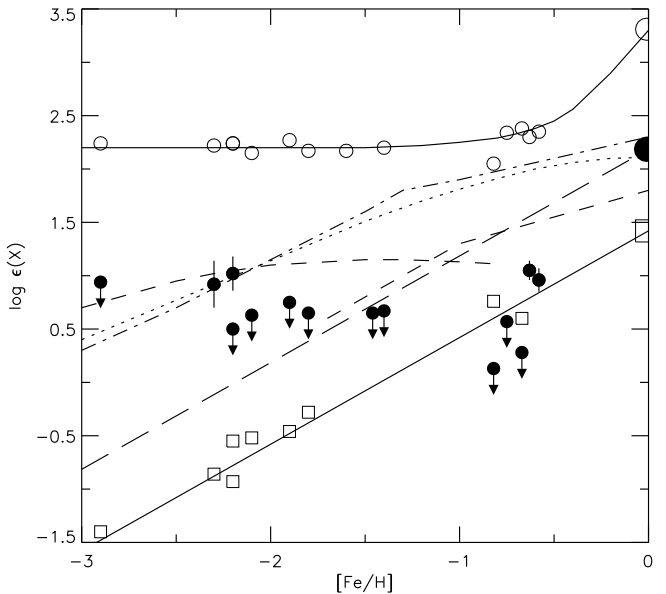


Fig. 9. Abundances of lithium and beryllium as a function of $[\text{Fe}/\text{H}]$ for 9 halo stars from Smith et al. (1998) and 5 disk stars from the present paper. Open circles indicate the total Li abundance and filled circles the ${}^6\text{Li}$ abundance or an upper limit. Open squares refer to the Be abundance adopted from Gilmore et al. (1992) and Boesgaard et al. (1999b). The big symbols indicate meteoritic abundances from Anders & Grevesse (1989). The upper full drawn line is a fit to the ‘Spite plateau’ of lithium abundances for $[\text{Fe}/\text{H}] < -1.5$ and to the upper envelope of the Li abundance distribution for disk stars (see fig. 7 of Lambert et al. 1991). The lower full drawn line is a linear fit to the beryllium abundances with a slope of one, and the long-dashed line shows the corresponding relation for ${}^6\text{Li}$ if ${}^6\text{Li}/\text{Be} = 5.8$ as found in meteorites and as predicted from spallation of CNO nuclei by high energy cosmic rays. The dotted line represents the evolution of ${}^6\text{Li}$ in the model of Fields & Olive (1999a,b), the dashed-dotted line the model of Vangioni-Flam et al. (1999) and the short-dashed lines refer to the model of Yoshii et al. (1997) for the halo and disk, respectively

energy’ refers to energies close to the threshold energies of the spallation and fusion reactions.) A key point about this component is that the He, C, and O abundances of the ejecta are considered to be much higher than in the halo interstellar medium and, then, the dominant spallation process is between (say) O in the ejecta and protons in the interstellar gas whereas in the standard picture (Fields & Olive 1999a,b) the leading process is between protons in the cosmic rays and (say) O in the interstellar gas. In Fig. 9, we show predictions (dashed-dotted line) from a model adjusted to fit the measured ${}^6\text{Li}$ abundances of the two halo stars. This model predicts a ${}^6\text{Li}$ abundance at $[\text{Fe}/\text{H}] = 0$ that exceeds slightly the solar abundance.

The close correspondence between the two predictions is unlikely to be a fair measure of the uncertainties in predicting the ${}^6\text{Li}$ abundance of $1 M_{\odot}$, $[\text{Fe}/\text{H}] \simeq -0.6$ disk stars starting from either the solar ${}^6\text{Li}$ abundance or the ${}^6\text{Li}$ abundance of halo stars. While the ${}^6\text{Li}$ contribution from spallation by galactic high-energy cosmic rays is rather well constrained by the observed Be abundance, there are no comparable constraints on the contributions of the fusion reactions and of spallation by low energy cosmic rays.

That the range of permissible predictions is wider than perhaps suggested by the above two recent papers is suggested by an earlier discussion by Yoshii et al. (1997). The prediction shown in Fig. 9 is from their Fig. 2¹ for a model that considers high-energy cosmic rays with cosmic ray protons and alphas spallating interstellar C,N, and O nuclei as well as $\alpha + \alpha$ reactions. The cosmic ray flux was assumed to increase with decreasing metallicity. Different models are adopted for the halo and disk. This model predicts a rather shallow decline of the ${}^6\text{Li}$ abundance in the halo, and a steeper increase in the disk. Almost all of the ${}^6\text{Li}$ in the halo is the product of the $\alpha + \alpha$ reactions. The prediction fails by about 0.4 dex to account for the solar ${}^6\text{Li}$ abundance, so that the discrepancy between prediction and observation for our disk stars might be larger for a revised model that did reproduce the solar ${}^6\text{Li}$ abundance.

Our old disk stars with detectable ${}^6\text{Li}$ have Li abundances slightly in excess of the Spite plateau. If, as standard models of pre-main sequence and main sequence evolution predict, the depletion of ${}^7\text{Li}$ has been extremely slight, we may use the observed abundance and the prediction that cosmic ray production of the Li isotopes gives an isotopic ratio ${}^7\text{Li}/{}^6\text{Li} \simeq 1.5$ to estimate the contribution of ${}^6\text{Li}$ from cosmic rays. Consider HD 68284 with a Li abundance $\log\epsilon(\text{Li}) = 2.35$. This is higher than the Spite plateau of $\log\epsilon(\text{Li}) = 2.21$ (Smith et al. 1998). On the assumption that plateau stars have not depleted Li, the increase of Li in HD 68284 corresponds to $\text{Li} \simeq 60$ on the scale $H = 10^{12}$. If cosmic rays were entirely responsible for this increase, a division ${}^7\text{Li} \simeq 36$ and ${}^6\text{Li} \simeq 24$ is appropriate for a production ratio ${}^7\text{Li}/{}^6\text{Li} \simeq 1.5$. The Be abundance implies ${}^6\text{Li} \simeq 30$ so that at this metallicity spallation rather than fusion reactions may be dominant. The observed ${}^6\text{Li}$ abundance is ${}^6\text{Li} \simeq 10$. (HD 130551 provides similar figures.) Given that ${}^6\text{Li}$ has assuredly been depleted to at least a modest extent, this elementary dissection of the observed Li abundance reveals no obvious difficulty with a cosmic ray contribution to the Li isotopes.

Recently, Ryan et al. (1999) have argued on the basis of lithium abundances of Spite plateau stars in the range $-3.5 < [\text{Fe}/\text{H}] < -2.3$ that the plateau has a metallicity

¹ In converting $[\text{O}/\text{H}]$ to $[\text{Fe}/\text{H}]$ we have adopted $[\text{O}/\text{H}] = [\text{Fe}/\text{H}] + 0.5$ for $[\text{Fe}/\text{H}] < -1.0$ and $[\text{O}/\text{H}] = 0.5 [\text{Fe}/\text{H}]$ for $[\text{Fe}/\text{H}] > -1.0$

dependence due to the manufacture of the Li isotopes by cosmic rays. They consider the primordial abundance to be $\log\epsilon(\text{Li}) \simeq 2.00$ at $[\text{Fe}/\text{H}] = -3.5$. If Smith et al.'s T_{eff} -scale is adopted, this abundance is raised to be about 2.12 according to 4 stars common to both analyses. This and Ryan et al.'s metallicity dependence predict HD 68284 to have a Li abundance of 2.44 which is similar to the observed value of 2.35. Relative to a plateau of 2.12, the observed abundance implies cosmic rays have added Li in the proportion ${}^7\text{Li} = 54$ and ${}^6\text{Li} = 36$ which are consistent with our observations provided that ${}^6\text{Li}$ has been depleted by about 0.6 dex. At some point in the evolution of the Galaxy, sources (presumably stellar) contributed ${}^7\text{Li}$ with little or no ${}^6\text{Li}$ in order to raise the ${}^7\text{Li}/{}^6\text{Li}$ ratio to the solar ratio of 12.5. Inclusion of such a contribution in the above argument reduces the ${}^6\text{Li}$ inferred from the increase in Li abundance over the plateau's value.

The preceding argument may be inverted: the predicted growth of ${}^6\text{Li}$ with $[\text{Fe}/\text{H}]$ may be used to infer the ${}^7\text{Li}$ abundance. For example, the models proposed by Fields & Olive, and Vangioni-Flam et al. predict a ${}^6\text{Li}$ abundance in the ISM at the birth of HD 68284 and HD 130551 of about 120, a factor of 12 greater than observed. Assuming again a production ratio of ${}^6\text{Li}/{}^7\text{Li} = 1.5$ the attendant ${}^7\text{Li}$ abundance is 180. Added to the primordial ${}^7\text{Li}$ abundance of 160 this implies a total ${}^7\text{Li}$ abundance of 340 ($\log\epsilon({}^7\text{Li}) = 2.53$), a value considerably greater than the observed value of about 200. The obvious implications are that either the predicted ${}^6\text{Li}$ abundance is greatly overestimated or ${}^7\text{Li}$ has been depleted by about 0.2 dex. In sharp contrast, Yoshii et al.'s prediction is a ${}^6\text{Li}$ abundance of about 30 providing a total ${}^7\text{Li}$ abundance of 205 or $\log\epsilon(\text{Li}) = 2.31$, in excellent agreement with the observed ${}^7\text{Li}$ abundances of HD 68284 and HD 130551. This model fails, however, to account for the meteoritic ${}^6\text{Li}$ abundance by a large amount.

6. Concluding Remarks

It is presently impossible to refine our conclusions because understanding of Li-depletion, especially of ${}^6\text{Li}$ -depletion, is poor. This is unfortunate as there is a tantalizing hint from the few detections of ${}^6\text{Li}$ with the support of the greater suite of upper limits to the ${}^6\text{Li}$ abundance that the growth of the ${}^6\text{Li}$ abundance in the Galaxy up to the metallicity of the old disk ($[\text{Fe}/\text{H}] \sim -0.5$) may have been very slight, a result in conflict with the most recent models of ${}^6\text{Li}$ chemical evolution but in agreement with a model proposed by Yoshii et al. (1997). This tentative suggestion is dependent on the absence of severe ${}^6\text{Li}$ -depletion in our disk stars.

Further progress will need additional observations of ${}^6\text{Li}$ in halo and disk stars. Such observations for extremely metal-poor stars, say $[\text{Fe}/\text{H}] < -3$, will require a high-resolution spectrograph on an extremely large telescope. More common instrumentation will be adequate for ex-

panding the sample of more metal-rich halo and disk stars with a known ${}^6\text{Li}$ abundance and, in this case, a very large sample of stars may be needed to map out the upper envelope to the ${}^6\text{Li}$ vs [Fe/H] relation which with the corresponding ${}^7\text{Li}$ vs [Fe/H] envelope may suffice to determine empirically the evolution of the ${}^7\text{Li}/{}^6\text{Li}$ ratio. A by-product of the survey will be measures of the range of ${}^6\text{Li}$ -depletions experienced by low mass stars of differing metallicity that will serve as grist for the theoreticians' mills.

Acknowledgements. This research has been supported in part by the Danish Natural Science Research Council, the US National Science Foundation (grant 96-18414) and the Robert A. Welch Foundation of Houston, Texas.

References

Anders E., Grevesse N. 1989, *Geochim. Cosmochim. Acta* 53, 197

Andersen J., Gustafsson B., Lambert D. 1984, *A&A* 136, 65

Asplund M., Nordlund Å., Trampedach R., Stein R.F. 1999, *A&A* 346, L17

Bevington P.R., Robinson D.K. 1992, *Data reduction and error analysis for the physical sciences*, McGraw-Hill, p.212

Boesgaard A.M., King J.R., Deliyannis C.P., Vogt S.S. 1999a, *AJ* 117, 492

Boesgaard A.M., Deliyannis C.P., King J.R., Ryan S.G., Vogt S.S., Beers T.C. 1999b, *AJ* 117, 1549

Brault J.W., Müller E.A. 1975, *Solar Phys.* 41, 43

Cayrel R., Spite M., Spite F., E. Vangioni-Flam, Cassé M., Audouze J. 1999a, *A&A* 343, 923

Cayrel R., Lebreton Y., Morel P. 1999b, in *Connecting the distant Universe with the local fossil record*, eds. M. Spite and F. Crifo, Kluwer (in press, astro-ph/9902068)

Chaboyer B. 1994, *ApJ* 432, L47

Copi C.J., Schramm D.N., Turner M.S. 1997, *Phys. Rev. D* 55, 3389

Dravins D. 1987, *A&A* 172, 211

D'Odorico s., Avila S., Molaro P. 1989, *ESO Messenger* 58, 58

Duncan D.K., Primas F., Rebull L.M., Boesgaard A.M., Deliyannis C.P., Hobbs L.M., King J.R., Ryan S.G. 1997, *ApJ* 488, 338

ESA 1997, *The Hipparcos and Tycho Catalogues*, ESA SP-1200

Edvardsson B., Andersen J., Gustafsson B., Lambert D.L., Nissen P.E., Tomkin J. 1993, *A&A* 275, 101

Fields B.D., Olive K.A. 1999a, *ApJ* 516, 797

Fields B.D., Olive K.A. 1999b, *New Astronomy* (in press) (astro-ph/9811183)

Garcí López R.J., Lambert D.L., Edvardsson B., Gustafsson B., Kiselman D., Rebolo R. 1998, *ApJ* 500, 241

Gilmore G., Gustafsson B., Edvardsson B., Nissen P.E. 1992, *Nature* 357, 379

Gray D.F. 1978, *Solar Phys.* 59, 193

Gray D.F. 1992, *The observation and analysis of stellar photo-spheres*, Cambridge University Press, p. 368

Hobbs L.M., Thurburn J.A. 1994, *ApJ* 428, L25

Hobbs L.M., Thurburn J.A. 1997, *ApJ* 491, 772

Israelian G., García López R.J., Rebolo R. 1998, *ApJ* 507, 805

Kurucz R.L. 1993, CD-ROM # 1, 13, 18

Kurucz R.L., Furenlid I., Brault J., Testerman L. 1984, *Solar Flux Atlas from 296 to 1300 nm*, National Solar Observatory, Sunspot, New Mexico

Lambert D.L., Heath J.E., Edvardsson B. 1991, *MNRAS* 253, 610

Lemoine M., Ferlet R., Vidal-Madjar A. 1995, *A&A* 298, 879

Matteucci F., d'Antona F., Timmes F.X. 1995, *A&A* 303, 460

Maurice E., Spite F., Spite M. 1984, *A&A* 132, 278

Müller E.A., Peytremann E., De La Reza R. 1975, *Solar Phys.* 41, 53

Nave G., Johansson S., Learner R.C.M., Thorne A.P., Brault J.W. 1995, *ApJS* 94, 221

Pinsonneault M.H., Deliyannis M.P., Demarque P. 1992, *ApJS* 78, 179

Pinsonneault M.H., Narayanan V.K., Steigman G., Walker T.P. 1998 in *Proceedings of the 10th Cambridge Workshop on Cool Stars, Stellar Systems and the Sun*, eds. J. Bookbinder and B. Donahue (in press)

Ramaty R., Kozlovsky B., Lingenfelter R.E. 1996, *ApJ* 456, 525

Ryan S.G., Norris J.E., Beers T.C. 1999, *ApJ* (submitted)

Smith V.V., Lambert D.L., Nissen P.E. 1993, *ApJ* 408, 262

Smith V.V., Lambert D.L., Nissen P.E. 1998, *ApJ* 506, 405

VandenBerg D.A., Swenson F.J., Rogers F.J., Iglesias C.A., Alexander D.R. 1999 (in preparation)

Vangioni-Flam E., Cassé M., Fields B.D., Olive K.A. 1996, *ApJ* 468, 199

Vangioni-Flam E., Cassé M., Cayrel R., Audouze J., Spite M., Spite F. 1999 (Preprint, astro-ph/9811327)

Woosley S.E., Weaver T.A. 1995, *ApJS* 101, 181

Yoshii Y., Kajino T., Ryan S.G. 1997, *ApJ* 485, 605